

Nonlinear optical properties of a channel waveguide produced with crosslinkable ferroelectric liquid crystals

Valentina S. U. Fazio *, Sven T. Lagerwall

*Department of Microelectronics and Nanoscience, Liquid Crystal Physics,
Chalmers University of Technology & Göteborg University, SE-41296 Göteborg, Sweden*

Vismant Zauls, Sigurd Schrader

Institute of Physics, University of Potsdam, D-14469 Potsdam, Germany

Philippe Busson, Anders Hult

Department of Polymer Technology, Royal Institute of Technology, SE-10044, Stockholm, Sweden

Hubert Motschmann

Max-Planck-Institute of Colloids and Interfaces, D-14476 Golm/Potsdam, Germany

Abstract

A binary mixture of ferroelectric liquid crystals (FLCs) was used for the design of a channel waveguide. The FLCs possess two important functionalities: a chromophore with a high hyperpolarizability β and photoreactive groups. The smectic liquid crystal is aligned in layers parallel to the glass plates in a sandwich geometry. This alignment offers several advantages, such as that moderate electric fields are sufficient to achieve a high degree of polar order. The arrangement was then permanently fixed by photopolymerization which yielded a polar network possessing a high thermal and mechanical stability which did not show any sign of degradation within the monitored period of several months. The linear and nonlinear optical properties have been measured and all four independent components of the nonlinear susceptibility tensor \bar{d} have been determined. The off-resonant d -coefficients are remarkably high and comparable to those of the best known inorganic materials. The alignment led to an inherent channel waveguide for p-polarized light without additional preparation steps. The photopolymerization did not induce scattering sites in the waveguide and the normalized losses were less than 2 dB/cm. The material offers a great potential for the design of nonlinear optical devices such as frequency doublers of low power laser diodes.

PACS number(s):

61.30.Gd (orientational order of liquid crystals; electric and magnetic field ef-

*e-mail: fazio@fy.chalmers.se

fects on order)
42.65.Ky (harmonic generation, frequency conversion)
42.82.Et (waveguides, couplers, and arrays)

1 Introduction

Organic materials have a great inherent potential for nonlinear optical (NLO) devices, such as frequency doublers and a variety of fast switching devices. This potential has been early recognized. Meanwhile there is a sound understanding of the correlation between the molecular structure and the resulting nonlinear optical properties. Many NLO chromophores with a remarkably high hyperpolarizability β have been synthesized. At present not the availability of suitable chromophores is the decisive hurdle for efficient devices, but the fabrication of suitable structures which have to simultaneously fulfill many criteria. Preparation schemes such as the Langmuir-Blodgett (LB) technique [1, 2] or poled polymers [3] lead to an unwanted intrinsic dilution of the active moiety within a matrix and in addition these films usually possess a low thermal or mechanical stability.

The figure of merit of all devices based on second-harmonic effects is given by the ratio d_{eff}^2/n^3 , where d_{eff} is the effective reduced nonlinear optical susceptibility and n the refractive index of the material. The oriented gas model [4] provides a relation between molecular and macroscopic quantities. It states that d_{eff} is proportional, in first approximation, to the number density of the NLO chromophores and to the orientational average, $\langle \beta \rangle$, of the molecular nonlinear hyperpolarizabilities. A maximization of d_{eff} requires a chromophore with a large value of β arranged in a uniform fashion with a high degree of polar order and a high number density. These demands can be fulfilled by ferroelectric liquid crystals (FLCs). Sophisticated preparation techniques developed for deliberate controlling and manipulating the order in liquid crystal systems can be utilized for the design of a NLO device.

Liquid crystals (LCs) are ordered organic materials that intrinsically possess a high number density and a quadrupolar order, but in general not a dipolar one [5]. In chiral smectic C (SmC*) liquid crystals, or FLCs, however, the molecular symmetry allows a local dipolar order perpendicular to the director [6] which can be extended to the whole sample either by orienting all the molecular dipoles in an external electric field or by surface constraints like the one used in surface-stabilized FLCs (SSFLCs) [7] which are characterized by a macroscopic polarization in the field-free state and in which the director can be switched between two stable states (bistable). In absence of a sufficient external field, the molecules are arranged in a helical fashion proper of the chiral phase, which has D_∞ symmetry and which does not possess a macroscopic polarization.

A lot of effort has been invested in the last decade in the synthesis and characterization of FLCs [8–11] and FLC polymers [12–15] for second-harmonic generation (SHG). Recently, bent-shaped molecules with very high nonlinear optical hyperpolarizabilities have been synthesized [16]. Despite all these accomplishments, the low thermal and mechanical stability of these systems is

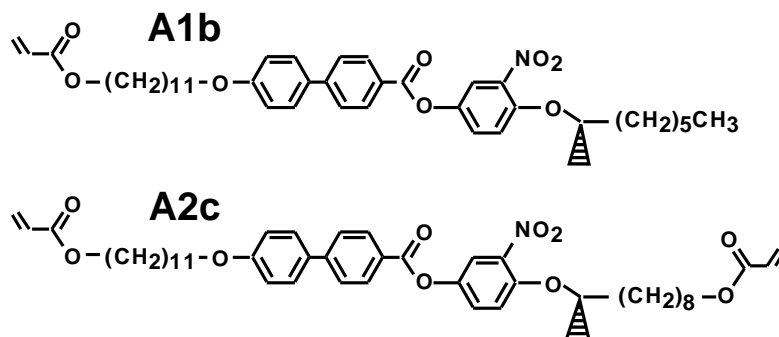


Figure 1: Ferroelectric liquid crystal monomers used in this experiment.

the reason why they did not gain a practical level of relevance. This issue is addressed in the present publication.

The FLCs used in our study possess a photoreactive group and can be crosslinked to give thermally and mechanically stable polar polymer networks [17–20]. The material can first be aligned by an electric field and then the polar order can be “frozen-in” by photopolymerization. The macroscopic polarization is now an intrinsic property of the polymer film which is neither ferroelectric nor truly liquid crystalline, but rather a *pyroelectric polymer* (PP), characterized by a macroscopic polarization which cannot be switched [19].

SHG in similar polymers has been studied in planar cells [18–21] where the glass plates were treated with unidirectionally rubbed polyimide for planar alignment (smectic layers standing perpendicular to the plates). Usually refractive indices and thickness of these aligning layers, such as polyimide, are unknown resulting in complications in the data interpretation. Moreover, because of the surface constraint, high electric fields are required to unwind the smectic helix.

Instead, we use quasi-homeotropic orientation. In this geometry all the (four) independent reduced second-order nonlinear susceptibilities can be determined, which is not the case in the planar geometry (see for instance [17]). There are a number of other advantages in this geometry as well. First of all, a very high quality of the alignment is obtained almost automatically when the layers are parallel to the glass plates and no aligning pre-coating is necessary. Second, there is essentially no threshold for the azimuthal motion of the director which continuously follows the electric field. An eventual small threshold could only result from surface pinning effects. Moreover, even the threshold for unwinding the smectic helix generally is lower in the quasi-homeotropic case than in the planar (bookshelf) one. Finally, in the homeotropic geometry the sample is a channel waveguide for p-polarized light without any additional preparation steps.

2 Material

The chemical structures of the FLC monomers used in this work are shown in Figure 1. The monomer A2c is terminated by two photoreactive end-groups that allow the formation of a stable polymeric network by photopolymerization [18].

compound	heating			cooling		
A1b	K 29 SmC*	58 SmA*	71 I	I 62 SmA*	50 SmC*	0 K [17]
A2c	K 29 SmC*	33 SmA*	39 I	I 34 SmA*	29 SmC*	8 K [18]
A1b/A2c 60/40				I 44 SmA*	31 SmC*	9 K this work

Table 1: Thermal transitions for the two ferroelectric liquid crystal monomers and the mixture used in this work (temperature in degrees Celcius; K = crystal, I = isotropic).

Within the polymer network the polar order of the monomeric system is permanently fixed (“frozen”). The monomeric FLC forms a highly twisted SmC* phase with a pitch of $0.4 \mu\text{m}$ [22] and therefore a fairly high DC electric field (more than $3 \text{ V } \mu\text{m}^{-1}$) is required to unwind the helix. The monomer **A1b** possesses only a single photoreactive end-group and only side-chain polymers are obtained after photopolymerization, but its helix can be unwound by a DC electric field of a few hundred $\text{mV } \mu\text{m}^{-1}$ in planar cells [17]. Both monomers possess a quite large spontaneous polarization (about 190 nC cm^{-2} at room temperature) [22].

In this work a mixture of 60% **A1b** and 40% **A2c** was used which combines the desired features of both monomeric systems: the low voltage to unwind the helix and establish a homogeneously polarised state and the possibility to freeze it by formation of a stable polymer network. The photopolymerization was enabled by adding a very small quantity (less than 1% in weight) of the photoinitiator Lucirin TPO (BASF) to the mixture. The phase behavior of the individual monomers and of the mixture is listed in Table 1.

3 Sample preparation

The geometry of the cell is shown in Figure 2. The bottom plate is equipped with two parallel ITO electrodes with $100 \mu\text{m}$ gap patterned by photolithography. No special surface treatments were used. The two plates were spaced with polyester films (Mylar) of various thickness.

The cells were inserted into a polarising microscope equipped with a hot stage and filled with the FLC mixture in the isotropic phase. During cooling to room temperature a small low-frequency AC electric field ($0.1\text{-}0.2 \text{ V } \mu\text{m}^{-1}$) was applied across the electrodes, both to facilitate the desired smectic order and to measure the electrooptic response. By integrating the transient current on field reversal the spontaneous polarization P_s is obtained. The temperature dependence of P_s is shown in Figure 3. At room temperature a value of $\approx (190 \pm 20) \text{ nC cm}^{-2}$ was measured, which is in agreement with the values found for the single monomers [22].

At room temperature a DC electric field ($\approx 50 \text{ mV } \mu\text{m}^{-1}$) was applied to unwind the smectic helix and orient the FLC molecular dipole moments in the electrode gap (see Figure 4). Since the gap between the electrodes is larger than the cell size by an order of magnitude, the electric field inside the channel is approximately horizontal and edge effects can be neglected. As a result a macroscopic domain of uniform orientation was formed between the electrodes. The samples were then irradiated with UV light. The photopolymerization led to the formation of a stable network: thereafter a temperature up to 160°C did not induce any phase transition and the polar order could not be reversed by

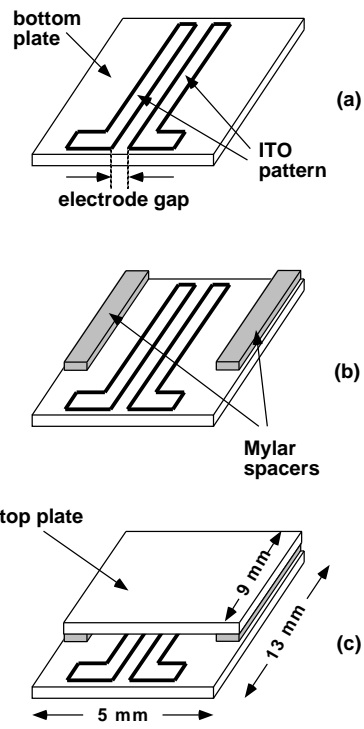


Figure 2: Manufacturing steps. (a) Patterning of the ITO electrodes. The gap between the electrodes is $100\ \mu\text{m}$ wide. The thickness of the ITO layer is about $15\ \text{nm}$. (b) Deposition of Mylar spacers of $13\ \mu\text{m}$ thickness. (c) The top glass plate is glued on, to complete the sandwich cell.

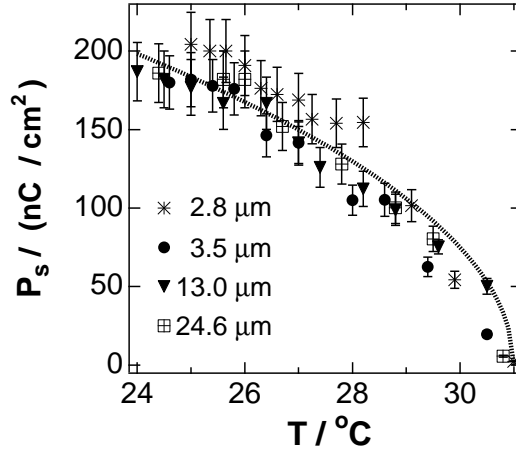


Figure 3: Spontaneous polarization as a function of temperature for the mixture used in this experiment. The markers represent P_s values measured in four cells of different thickness, the dashed line is a fit to the function $P_s = A\sqrt{B-T}$ [5], where A and B are fitting parameters ($A = 74.9 \text{ nC cm}^{-2} \text{ C}^{-\frac{1}{2}}$, $B = 31 \text{ }^\circ\text{C}$), and T is the temperature in degrees Celcius.

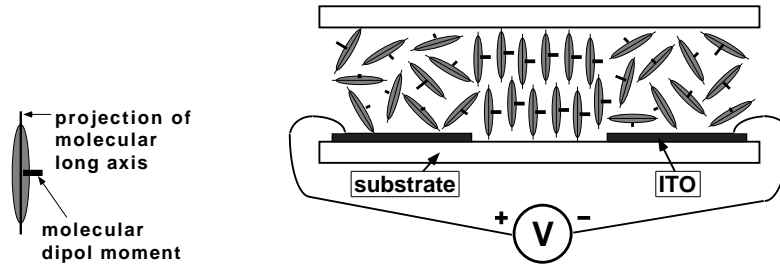


Figure 4: Cross section of a cell. In the gap between the electrodes the FLC material is oriented by the AC/DC field. The dipole moments are aligned along the cell plates perpendicular to the electrodes stripes. The smectic tilt plane is perpendicular to the page. In the channel between the electrodes we have a microscopic polarization whereas outside it we have a disordered non-polar state (the liquid crystalline disorder in these regions is somewhat exaggerated in the figure).

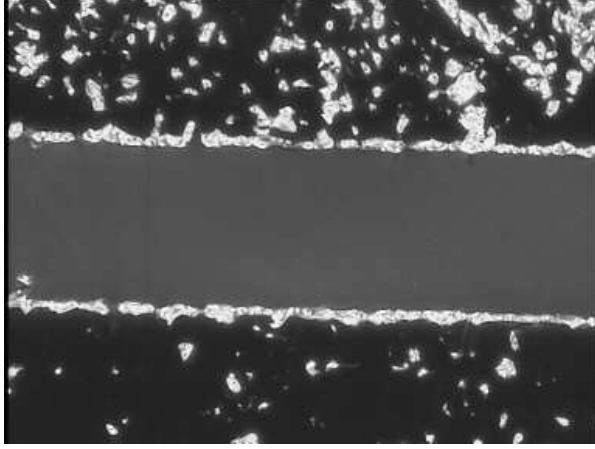


Figure 5: Micrograph of a cell after polymerization. The PP molecules are uniformly oriented in the channel between the electrodes. The cell thickness is $13\ \mu\text{m}$ and the electrode gap is $100\ \mu\text{m}$.

an electric field. In other words, the polar order induced by the external field had been frozen. The photopolymerization did not induce any defects visible by optical means and the alignment was uniform within the stripe. Figure 5 is a micrograph of a cell after photopolymerisation. The stripe appeared dark gray between crossed polarisers. Rotation of the sample between crossed polarizers did not essentially change any feature. This suggests that in such thick cell the smectic helix is not completely unwound and that the optic axis as well as the polarization is not completely homogeneous across the sample. Yet, we can consider the PP essentially homeotropically aligned.

4 Second-harmonic generation experiment

SHG requires noncentrosymmetry and thus can only occur within the channel region of our waveguide. Figure 6 shows the geometry and definition of the frame of reference for modelling SHG.

The unwound SmC* liquid crystal phase belongs to the C_2 symmetry group. The second-order reduced susceptibility tensor, \bar{d} , of this group contains four independent coefficients [3]:

$$\bar{d} = \begin{pmatrix} 0 & 0 & 0 & d_{14} & 0 & d_{16} \\ d_{16} & d_{22} & d_{23} & 0 & d_{14} & 0 \\ 0 & 0 & 0 & d_{23} & 0 & d_{14} \end{pmatrix}. \quad (1)$$

In the homeotropic geometry only s-to-s or p-to-s conversions are allowed [17]. The effective susceptibilities which govern the conversions can be expressed in terms of the components of the \bar{d} tensor as:

$$\text{s-to-s} \quad d_{\text{eff}} = d_{22}, \quad (2)$$

$$\text{p-to-s} \quad d_{\text{eff}} = d_{16} \cos^2 \theta + d_{23} \sin^2 \theta + 2d_{14} \sin \theta \cos \theta, \quad (3)$$

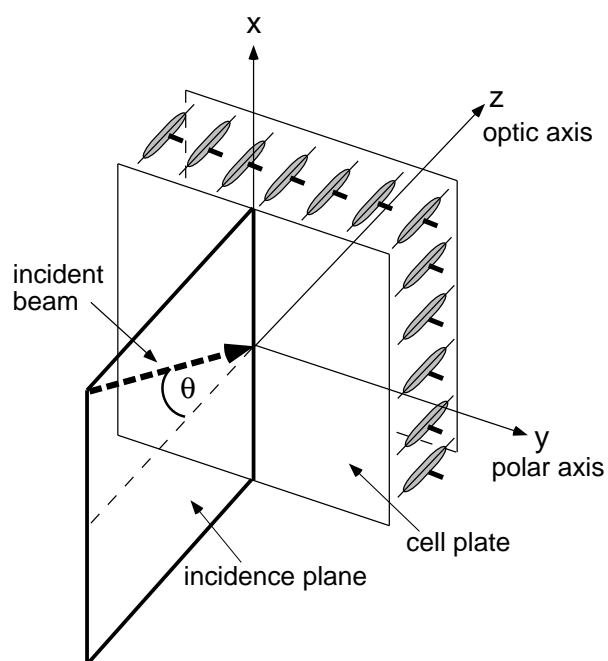


Figure 6: Geometry and definition of the coordinate system of the SHG experiment in the channel region. The macroscopic dipole moment of the polymer network is oriented along the y -axis, parallel to the glass plates. Although the director is not perfectly homogeneous across the cell, the effective optic axis is along z , perpendicular to the glass plates. θ is the internal incidence angle.

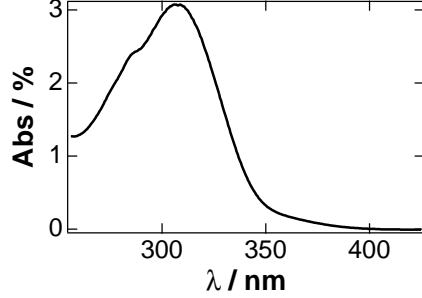


Figure 7: Adsorption spectrum of the mixture A1b/A2c 60/40 in chloroform solution 0.13 mM. The material is transparent at the wavelengths of the fundamental (1064 nm) and the second harmonic (532 nm) light.

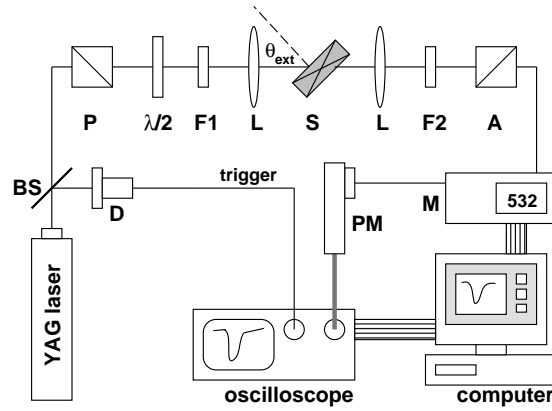


Figure 8: Setup for second-harmonic generation. P: polarizer; F1: visible-cut filter; L: lens; S: sample; θ_{ext} : external incidence angle; F2 fundamental-cut filter; A: analyzer; BS: beam splitter; D: detector; M: monochromator; PM: photomultiplier tube.

where θ is the fundamental light incidence angle at the glass/polymer interface (internal incidence angle, Figure 6) and $\theta_{\omega} = \theta_{2\omega} = \theta$. Eqn. 2 and 3 contain all the four independent coefficients of the \vec{d} -tensor. Hence, in homeotropic geometry, all four independent second-order reduced susceptibilities can be determined by measuring d_{eff} as a function of the incidence angle θ . This measurement was performed in transmission with a YAG laser (1064 nm, 35 ps, 10 Hz) in $13 \mu\text{m}$ thick cells. The material is transparent in the range of wavelengths of interest as can be concluded from the absorption spectrum shown in Figure 7. Therefore, our measurements yielded the off-resonant values of d_{eff} . A sketch of the SHG experiment is shown in Figure 8. The samples were rotated about the polar axis (y -axis in Figure 6) and the second-harmonic light intensity was recorded versus the rotation angle θ_{ext} . Due to the small size of the channel region (only $100 \mu\text{m}$ wide) the alignment is rather critical and we had to ensure that the goniometer axis of rotation coincides with the polar axis of the PP cell.

d_{22}	=	$(0.76 \pm 0.10) \text{ pm V}^{-1}$
d_{16}	=	$(0.63 \pm 0.09) \text{ pm V}^{-1}$
d_{23}	=	$(1.26 \pm 0.16) \text{ pm V}^{-1}$
d_{14}	=	$(0.13 \pm 0.02) \text{ pm V}^{-1}$

Table 2: The four independent d -coefficients as calculated from the fits in Figure 9.

The SHG intensities as function of the external angle of incidence are shown in Figure 9 for both s-to-s and p-to-s polarizations. The dots are the experimental values and the lines are fits [23] that yielded the values of the four independent d -coefficients listed in Table 2. The values are comparable to those of quartz due to the large molecular hyperpolarizabilities combined with the high degree of orientational order and the high number density of the active chromophores in our system. Some of the coefficients exceed the values measured in planar geometry by 30-50 % [21], which shows the superior features offered by the homeotropic alignment.

5 Waveguide characteristics

The structure is a channel waveguide for p-polarised light (TM modes). Assuming homeotropic alignment between the electrodes, the propagation characteristics of TM modes in the channel region are dominated by the extraordinary refractive index of the PP, n_e . On the other hands, outside the channel region p-polarised light will see a refractive index which is somewhere in between n_e and n_o . Since $n_e > n_o$ at all wavelengths (the values n_e and n_o are reported in the caption of Figure 9), TM modes are three-dimensionally confined in the channel region and no additional preparation processes are required to obtain this desired feature. Here again the homeotropic geometry is advantageous. The corresponding arrangement in planar cells, where the alignment is uniform in the whole cell, leads only to slab waveguides.

The losses for p-polarised light at 1064nm were measured by monitoring the output power at different lengths of the guide. *End-fire* coupling was used to excite waveguide modes. The transmitted power was first measured with the 9mm long waveguide. Then the guide was shortened to 4mm and the transmitted power was measured again using the very same arrangement. The loss coefficient was found to be

$$\alpha = (1.07 \pm 0.95) \text{ dB cm}^{-1}. \quad (4)$$

The upper limit of the losses is on the order of 2 dB/cm which meets already the demands imposed by nonlinear optical devices, as for instance frequency doublers in waveguide format, and demonstrates the inherent potential of FLCs. Most devices require only an interaction length of 1–2mm. It is also remarkable that the scattering characteristics did not change with the polymerization even though this step is always accompanied by changes in the molecular arrangement. It is known for instance from LB films that polymerization induces scattering sites as the result of the formation of additional bonds. Apparently the high fluidity of the monomeric LC system is capable to heal these types of distortions.

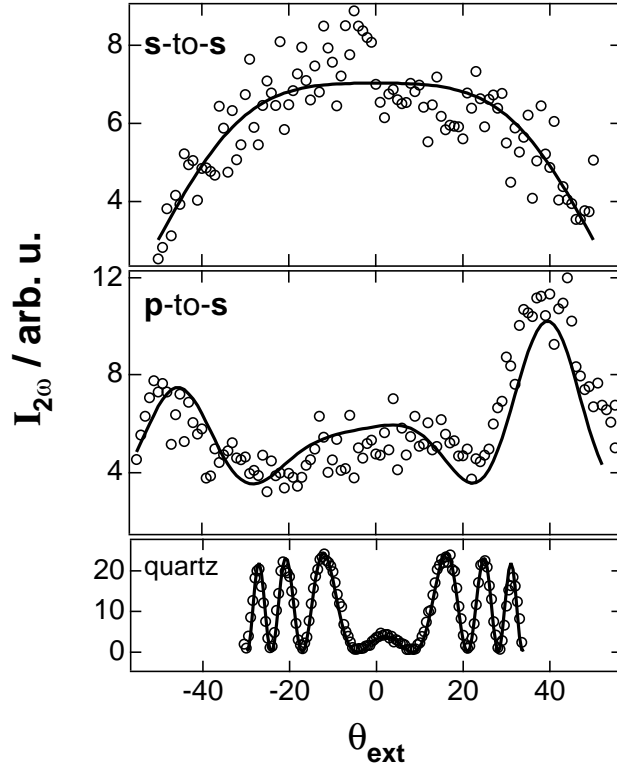


Figure 9: Second-harmonic light intensity versus external angle of incidence for s-to-s and p-to-s conversions, and for the quartz crystal of reference. The dots are the experimental values and the lines correspond to fits according to [23], with the following parameters: glass plate refractive indices, $n_g(\omega) = 1.46$ and $n_g(2\omega) = 1.50$; FLC ordinary refractive indices, $n_o(\omega) = 1.47$ and $n_o(2\omega) = 1.52$ [21]; FLC extraordinary refractive indices, $n_e(\omega) = 1.57$ and $n_e(2\omega) = 1.62$ [21]; cell thickness $13 \mu\text{m}$; second-order susceptibility of the quartz used for calibration, $d_{11} = (0.32 \pm 0.04) \text{ pm V}^{-1}$ [24]. The values of the second-order reduced susceptibilities calculated from the fits are listed in Table 2.

There are two kinds of scattering losses in optical waveguides [25]: volume and surface scattering losses. Volume scattering is caused by defects in the waveguide volume (scattering centers) and depends on the number of defects and on their relative dimension to the wavelength of the light, λ . If the defects are small compared to λ , the losses due to volume scattering will be negligible compared to the ones due to surface scattering. This is the case in our samples: no defects were observed in the channel region either before or after polymerization, and no scattering of light due to the polymerization was observed.

Surface scattering losses occur at each reflection of the traveling wave in the waveguide [25]. Even if the surfaces are very smooth this kind of losses can be significant. The surface scattering loss coefficient in a symmetric waveguide in the approximation of well-confined modes is [26]:

$$\alpha_s = A^2 \frac{1}{2} \frac{\cos^3(\frac{\pi}{2} - \theta_m)}{\sin(\frac{\pi}{2} - \theta_m)} \frac{1}{t}, \quad (5)$$

where

$$A = \sqrt{2} \frac{4\pi n_m}{\lambda} \sigma_{\text{gf}}. \quad (6)$$

θ_m and n_m are the internal reflection angle and the refractive index of the m -th guided mode, respectively; t is the waveguide thickness; λ is the vacuum wavelength; σ_{gf} is the variance of the surface roughness at the glass/film interface.

To measure the roughness of the polymer film, a hydrophobic quartz glass plate was used as top plate for a $13 \mu\text{m}$ thick cell. Being hydrophobic, the plate could be removed without damaging the PP [27]. The polymer surface was then studied with atomic force microscopy. Several scans were made and the variance of the surface roughness in the channel region was measured, $\sigma_{\text{gf}} = 2.3 \text{ nm} \pm 1.0 \text{ nm}$. A representative AFM picture is shown in Figure 10.

The surface appears extremely smooth, and the roughness is almost entirely due to that of the quartz glass plate (which was previously measured with an Alpha-step). Taking into account all the TM modes supported by the $13 \mu\text{m}$ thick waveguide and the variance of the surface roughness just measured, the total surface loss coefficient could be calculated:

$$\alpha_{\text{s,TOT}} = (0.42 \pm 0.23) \text{ dB cm}^{-1}. \quad (7)$$

This means that the optical losses are mainly due to the coupling of the light in and out of the waveguide.

6 Conclusions

The fabrication of a channel waveguide on the basis of ferroelectric liquid crystals has been demonstrated. The FLC monomers can be quasi-homeotropically aligned by an external electric field, resulting in a high degree of order and number density. This order can be frozen-in by photopolymerization which yields a network with a high mechanical and thermal stability. The measured losses of the waveguide are about 1–2 dB/cm (normalized to the fraction of the power

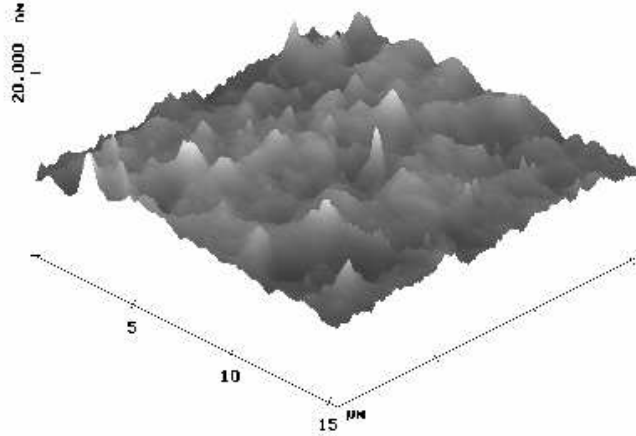


Figure 10: AFM scan of the polymer surface in the channel region. The variance of the surface roughness is $\sigma_{\text{gf}} = 2.3 \text{ nm} \pm 1.0 \text{ nm}$.

guided in the organic material) and already meet the requirements imposed by nonlinear optical devices. The network formation does not lead to a degradation of the quality of the waveguide and the fluidity in the LC system heals distortions caused by the formation of new chemical bonds. All independent nonlinear optical coefficients have been determined and the high number density of the chromophores and their high degree of orientational order lead to remarkably high d values.

The use of photopolymerizable FLCs offers rather appealing advantages compared to the established preparation techniques such as Langmuir-Blodgett films or poled polymers. Due to intrinsic peculiarities of these techniques the number density remains rather low with only moderate levels of orientational order. The FLC system does not suffer from dilution of the chromophores and exhibits higher degree of orientational order. The preparation techniques to manipulate order in LC systems are fairly sophisticated and allow the design of nonlinear optical devices such as frequency doublers of low power diodes or opto-opto switches based on cascading $\chi^{(2)}$ interactions. Critical issues, as for instance the problem of phase-matching or the problem arising from a small overlap integral in waveguide structures, have to be duly considered in this new class of materials. With the possibility of locally controlling the polar order, it seems that FLCs have a great potential in this area.

7 Acknowledgments

Dr. T. Henning from the Swedish Nanometer Laboratory is gratefully acknowledged for the production of the photolithography masks used to make the electrode patterns. The authors are grateful to Dr. S. Leporatti and M. Schneider for the AFM images. Valentina S. U. Fazio and S. T. Lagerwall acknowledge the TMR European programme (contract number ERBFMNICT983023) and the Swedish Foundation for Strategic Research for financial support. P. Busson acknowledges the financial support from the Swedish Research Council for Engineering Science (TFR, grant 95-807).

References

- [1] M. C. Petty. *Langmuir-Blodgett films: an introduction*. Cambridge University Press, 1996.
- [2] A. Ulman. *An introduction to ultrathin organic films: from Langmuir-Blodgett to self-assembly*. Academic Press Boston, 1991.
- [3] P. N. Prasad and D. J. Williams. *Introduction to nonlinear optical effects in molecules and polymers*. John Wiley & Sons, 1991.
- [4] H. Motschmann, T. Penner, N. Armstrong, and M. Enzenyilimba. *J. Phys. Chem*, 97:3933, 1993.
- [5] P. G. de Gennes. *The physics of liquid crystals*. Oxford University Press, 1974.
- [6] R. B. Meyer, L. Liebert, L. Strzeleki, and P. Keller. *J. Physique*, 36:L69, 1975.
- [7] N. Clark and S. T. Lagerwall. *Appl. Phys. Lett.*, 36:899, 1980.
- [8] D. M. Walba, M. Blanca Ros, N. A. Clark, R. Shao, K. M. Johnson, M. G. Robinson, J. Y. Liu, and D. Doroski. *Mol. Cryst. Liq. Cryst.*, 198:51, 1991.
- [9] D. M. Walba, M. Blanca Ros, T. Sierra, J. A. Rego, N. A. Clark, R. Shao, M. D. Wand, R. T. Vohra, K. E. Arnett, and S. P. Velsco. *Ferroel.*, 121:347, 1991.
- [10] D. M. Walba, D. J. Dyer, P. L. Cobben, T. Sierra, J. A. Rego, C. A. Liberko, R. Shao, and N. A. Clark. *Ferroel.*, 179:211, 1996.
- [11] J.-Y. Liu, M. G. Robinson, K. M. Johnson, D. M. Walba, M. Blanca Ros, N. A. Clark, R. Shao, and D. Doroski. *J. Appl. Phys.*, 70(7):3426, 1991.
- [12] H. Kapitza, R. Zentel, R. J. Twieg, C. Nguyen, S. U. Vallerien, F. Kremer, and C. G. Wilson. *Adv. Mater.*, 2:539, 1990.
- [13] E. Wischerhoff, R. Zentel, M. Redmond, and O. Mondain-Monval. *Macromol. Chem. Phys.*, 195:1593, 1994.
- [14] J. Naciri, B. R. Ratna, S. Baral-Tosh, P. Keller, and R. Shashidhar. *Macromol.*, 28:5274, 1995.

- [15] M. Svensson, B. Helgee, K. Skarp, and G. Andersson. *J. Mater. Chem.*, 8:353, 1998.
- [16] R. Macdonald, F. Kentischer, P. Warnik, and G. Heppke. *Phys. Rev. Lett.*, 81(20):4408, 1998.
- [17] David Sparre Hermann. *Interaction of light with liquid crystals*. PhD thesis, Göteborg University and Chalmers University of Technology, 1997.
- [18] M. Trollsås, C. Orrenius, F. Sahlén, U. W. Gedde, T. Norin, A. Hult, D. Hermann, P. Rudquist, L. Komitov, S. T. Lagerwall, and J. Lindström. *J. Am. Chem. Soc.*, 118:8542, 1996.
- [19] A. Hult, F. Sahlén, M. Trollsås, S. T. Lagerwall, D. S. Hermann, L. Komitov, P. Rudquist, and B. Stebler. *Liq. Crys.*, 20(1):23, 1996.
- [20] M. Trollsås, F. Sahlén, U. W. Gedde, A. Hult, D. Hermann, P. Rudquist, L. Komitov, S. T. Lagerwall, and B. Stebler. *Macromol.*, 29(7):2590, 1996.
- [21] M. Lindgren, D. S. Hermann, J. Örtegen, P.-O. Arntzen, U. W. Gedde, A. Hult, L. Komitov, S. T. Lagerwall, P. Rudquist, B. Stebler, F. Sahlén, and M. Trollsås. *J. Opt. Soc. Am. B*, 15(2):914, 1998.
- [22] D. S. Hermann, P. Rudquist, S. T. Lagerwall, L. Komitov, B. Stebler, M. Lindgren, M. Trollsås, F. Sahlén, A. Hult, U. W. Gedde, C. Orrenius, and T. Norin. *Liq. Crys.*, 24(2):295, 1998.
- [23] J. Jerphagnon and S. K. Kurtz. *M. J. Appl. Phys.*, 41(4):1667, 1970.
- [24] M. J. Weber. *CRC handbook of laser science and technology*, volume III: Optical materials. CRC Press Inc., Florida, 1986.
- [25] R. G. Hunsperger. *Integrated optics: theory and technology*. Springer-Verlag, third edition, 1991. Chapter 5.
- [26] P. K. Tien. *Appl. Opt.*, 10(11):2395, 1971.
- [27] Both monomers are amphiphilic, as they form monolayers at the air/water interface which can be deposited onto solid substrates with the Langmuir-Blodgett technique.